Nonlinear phenomena as observed in the ear canal and at the auditory nerve

P. F. Fahey
AT&T Bell Laboratories, Murray Hill, New Jersey 07974 and Department of Physics, University of Scranton, Scranton, Pennsylvania 18510

J. B. Allen
AT&T Bell Laboratories, Murray Hill, New Jersey 07974

(Received 11 April 1983; accepted for publication 5 September 1984)

We report here several measures of nonlinear effects in the mammalian ear made in the external auditory meatus and in single neurons of the auditory nerve. We have measured the $2f_1 - f_2$ and the $f_2 - f_1$ distortion products and we have found that (a) the neural distortion product threshold curve for $2f_1 - f_2$ mirrors the low-frequency side of the frequency threshold curve, (b) when the neural distortion product threshold curve of $2f_1 - f_2$ is plotted versus $\log(f_2/f_1)$ its slope is about 50 dB/oct and its intercept is 10–20 dB above the frequency threshold at the characteristic frequency CF, (c) substantial $2f_1 - f_2$ distortion was seen in all animals studied while the $f_2 - f_1$ distortion product was only rarely found at substantial levels, and (d) the distortion product pressure observed in the ear canal was at a level equal to that detected at threshold by the neural units under study. We have also made measurements of two-tone rate suppression thresholds using two new and consistent threshold paradigms. We find that (a) for high and intermediate characteristic frequency neural units the suppression threshold is independent of frequency and at a level of about 70 dB SPL, (b) the suppression above CF is much less than below CF, and (c) the tip of the frequency tuning curve can be suppressed by up to 40 dB by a low-frequency suppressor.

PACS numbers: 43.63.Pd, 43.63.Hx

INTRODUCTION

In this paper we study two separate measures of cochlear nonlinear response, namely, distortion products and two-tone suppression. First, we report on measurements of two-tone distortion products detected at the auditory nerve of the cat. We then compare these threshold distortion product measurements with the acoustic distortion pressure levels as detected in the external auditory meatus. We shall restrict ourselves to the two largest observable distortion products (DPs) which are at frequencies $2f_1 - f_2$ and $f_2 - f_1$ (where f_2 is the higher frequency of two input tone frequencies f_1 and f_2). For a recent review of psychophysically measured DPs see Goldstein *et al.*, 1978 and for discussion of physiological studies, especially in cats, see Kim *et al.*, 1980; Buunen and Rhode, 1978; Buunen *et al.*, 1977; Smoorenburg *et al.*, 1976; Goldstein and Kiang, 1968.

The approach taken here is to use neurons in the auditory nerve of the cat as threshold detectors of the distortion products $2f_1 - f_2$ and $f_2 - f_1$. By making our measurements at the neural rate threshold we have avoided the nonlinear saturation of the neural rate level function as a function of sound pressure level. Hence, we have been able to measure distortion products close to the lowest possible detectable levels and to extensively measure the dependence of their generation upon the frequencies of the primaries. Moreover, we have made measurements of the distortion products in the ear canal pressure contemporaneously with the neural measurements. This approach has allowed us to measure the distortion product amplitude in the ear canal under the constraint of a neural iso-threshold DP stimulus. We have found, for this case, that the level of the acoustic distortion product measured in the ear canal is sufficient to account for the observed excitation of the neural unit under study. The level of nonlinear acoustic distortion product seen in the ear canal is much greater than that seen when the acoustic driver is terminated with a 1-cm^3 acoustic cavity. In several animals we observed the $2f_1 - f_2$ DP at rather substantial (but reduced) levels up to 1 h postmortem, but we did not study the lability of the DP in a systematic way.

In parallel with the distortion product measures, we have measured neural two-tone rate suppression thresholds. In our studies of two-tone suppression, a subthreshold tone of one frequency is used to reduce or remove the detectability of a tone at the CF. Here we have determined the level of the input of a subthreshold tone (which, by itself, would not drive the neural unit above its spontaneous rate) which reduces the neural response to a suprathreshold CF tone to the neuron's spontaneous rate response. (For a review of two-tone suppression and other nonlinear phenomena, see Hall, 1981.)

We have made extensive measurements, using our modified criterion, of the frequency dependence of two-tone suppression thresholds, and these results appear to be somewhat different than the results previously reported in the literature. For suppressors above the characteristic frequency, we have found only small amounts of two-tone suppression. For CFs above 3 kHz and suppressor frequencies below CF, we find up to 40 dB of rate suppression at the unit's CF. Moreover, we have measured two-tone suppression on the same units as our measurements of distortion products in the hope that one nonlinear phenomenon could be related to the other. No quantifiable correlations have as of yet been observed between these two nonlinear measures.

 0001-4966/85/020599-14$00.80

I. METHODS

A. General

The data presented in this study have been obtained from 20 cats. From each animal we have characterized frequency threshold curves (FTCs) for more than 100 neural units along the auditory nerve during the 24- to 36-h experimental run. We are presenting data here that have come from animals with good thresholds ($\approx$15–30 dB SPL *re*: 20 μPa). Due to limitations of the upper frequency cutoff of our acoustic driver (25 kHz), our distortion product measurements were obtained only on units with characteristic frequencies (CFs) of less than 13 kHz.

Both the surgery necessary to gain access to the auditory nerve and the mechanical, electronic, and computing apparatus used in this study, have been described in detail by Allen (1983). Briefly, the animals were adults of body weight 2–5 kg, which were free of ear mites and middle ear infections. Access to the auditory nerve followed retraction of the cerebellum. The cochlear microphonic (CM) was monitored with a silver ball electrode apposed to the round window both before and after the skull opening and before and after the retraction of the cerebellum. Anesthesia was maintained with sodium pentobarbitol and was administered intraperitoneally as required to suppress a pinch reflex.

Both the electrical input to the acoustic driver (Sokolich, 1977) and the response measurements (from the calibrated probe microphone, from the CM electrode, and from the neural electrode) were under the control of a Data General S/200 Eclipse minicomputer. This system allowed us to measure a neural FTC, using the Kiang and Moxon paradigm (Liberman, 1978) in under 1 min. Moreover, we interleaved ear canal pressure measures with neural distortion product threshold measures in under 2 min. Under no condition were SPLs greater than 110 dB ever delivered to the animal. In fact, only briefly was the input greater than 80 dB SPL, as measured in the ear canal.

Our neural measurements proceeded as follows. A glass micropipette filled with 3M KCl (resistances between 10 MΩ and 30 MΩ) was inserted by manual micrometer adjustment into the auditory nerve. Thereafter, the position of the micropipette was under the control of a Burleigh "inch worm" PZT drive. Neural units were found by inputing a gated wideband noise search stimulus. Once found, the unit FTC was measured by scanning from high to low frequency while changing the input amplitude of a windowed 50-ms tone pip until the number of neural spikes generated during the tone interval was only one more than the number of spikes during an adjacent 50-ms silent interval. The locus of the points so obtained, in frequency-amplitude space, defines the FTC.

B. Distortion products

Given the FTC and, hence, the CF frequency f_{CF}, we then input an acoustic tone pip comprised of two frequencies, f_1 and f_2, where $f_2 > f_1$, such that either $2f_1 - f_2$ or alternatively $f_2 - f_1$ was at or slightly below the f_{CF}. The two tones have given pressure levels A_1 and A_2. Again, we used the Kiang and Moxon paradigm to determine the locus of acoustic stimulus points in the frequency-amplitude (f_1,A_1) plane such that the unit responded with one more spike during the driven interval than during the silent interval. This locus of points defines a distortion threshold curve (DTC). For most of the data curves presented here the pressure amplitude of f_1 and f_2 was approximately equal ($A_1 = A_2 = A$).

Effectively, our procedure is to calibrate an auditory neuron (by measuring its FTC) and then to use the response of this "calibrated" neuron to determine the acoustic level at each frequency to maintain an iso-rate neural DP response.

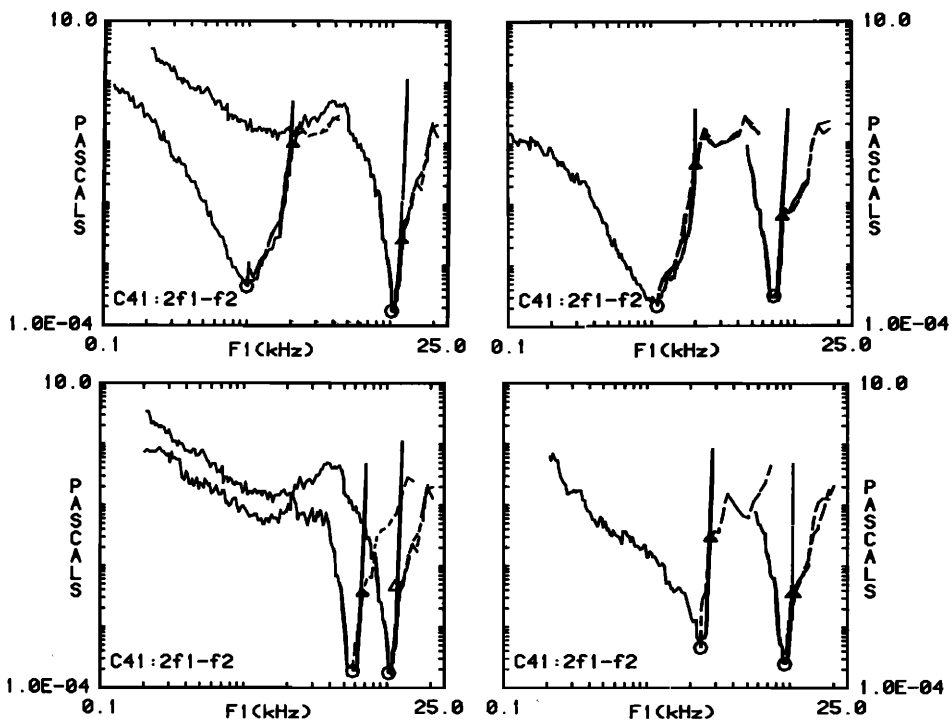

FIG. 1. This figure shows eight FTCs (solid lines) for cat 41 with the respective raw distortion data DTCs (dashed lines) of the unit. The DTC is defined in the text. With most units multiple DTC runs are shown. Also on the DTCs there is a triangle at the DTC–FTC intersection. Points on the DTC of lower frequency than the intersection point are not considered part of the DTC because the f_1 primary rather the distortion product is driving the unit.

In Fig. 1 we show several FTCs (solid lines) along with the units' $2f_1 - f_2$ DTCs (dashed lines). In each panel of the figure the amplitude of the distortion product has been held constant at the CF threshold. (If we were to shift the distortion product frequency from CF, we could then change the gain of our neural detector and hence change the amplitude of the distortion product that we are measuring.) We define the distortion product rate threshold as the smallest primary level which can generate a detectable DP response. Note that for any f_1 below the frequency of intersection of the DTC and the FTC, *both* the stimulus component at f_1 and the distortion product drive the unit. In each of the units of Fig. 1 the FTC–DTC intersection is marked with a triangle. In the figures that follow we call the level of the FTC–DTC intersection the distortion product rate threshold (DPT). Several of the units in Fig. 1 show multiple passes of the DTC.

The curves in our Fig. 1 are similar to curves in Buunen and Rhode (1978) (their Fig. 3) that defined the "maximum frequency separation for detectability of a CDT." Generally, their measure contains information that is similar to our DTCs, although the precise manner in which their amplitudes are measured differs.

Figures 2 and 3 show several FTCs with spline fitted DTCs. We averaged multiple DTC passes on the same unit by least squares fitted splines (Fox, 1976) to the total set of DTC points. In Fig. 2 we show cubic spline fits of $2f_1 - f_2$ DTCs. Shown in Fig. 3 are spline fits of $f_2 - f_1$ DTCs for the same animal.

C. Ear canal pressure measurements

The ear canal pressure was measured with a calibrated Bruel and Kjaer 1/2-in. microphone terminating a 2-cm-long probe tube. The tip of the probe tube was positioned to within 2–4 mm of the umbo. The same probe microphone was used to ascertain the level of distortion in the external auditory meatus and in a closed 1-cc acoustic cavity. In the acoustic cavity the level of the distortion product was always more than 70 dB below the primaries (near the distortion floor of the driver).

II. RESULTS

A. Neural

Because our detectors are neurons at threshold, the gains of these detectors are various. In order to account for these different gains, we can express the DTC relative to the gain of the detector (i.e., in most cases here, relative to the value of the FTC at CF). In Fig. 4(a) and (b) are two FTCs with DTCs in which the thresholds at CF are different. In Fig. 4(c) the DTCs are normalized by their respective FTCs at CF. We call the normalized DTC the relative distortion threshold curve (RDTC). Note that were we measuring a linear phenomenon the presentation of the data in this normalized way would be natural. For a phenomenon that is not linear, one might expect that a normalization by the detector threshold to some nonlinear function of that threshold would be the natural normalization. For example, if the $2f_1 - f_2$ were completely accounted for by the cubic term of a power series expansion in input amplitude A, then the proper normalization for us to use would be relative to the cube root of the threshold at CF. As can be seen from Fig. 4(c) and from previous works of others (Goldstein and Kiang, 1968 and Buunen and Rhode, 1978), the normalization by the threshold at CF that we chose seems to best reflect the amplitude dependence of the $2f_1 - f_2$ signal. In Fig. 4(d), we show the effect of changing the gain of the detector by displacing the $2f_1 - f_2$ tone from the CF. Notice that the DTC generated under these conditions is several dB higher than the DTC generated at a frequency equal to CF. Likewise, the threshold (the value of the FTC) of the detector is also higher. In

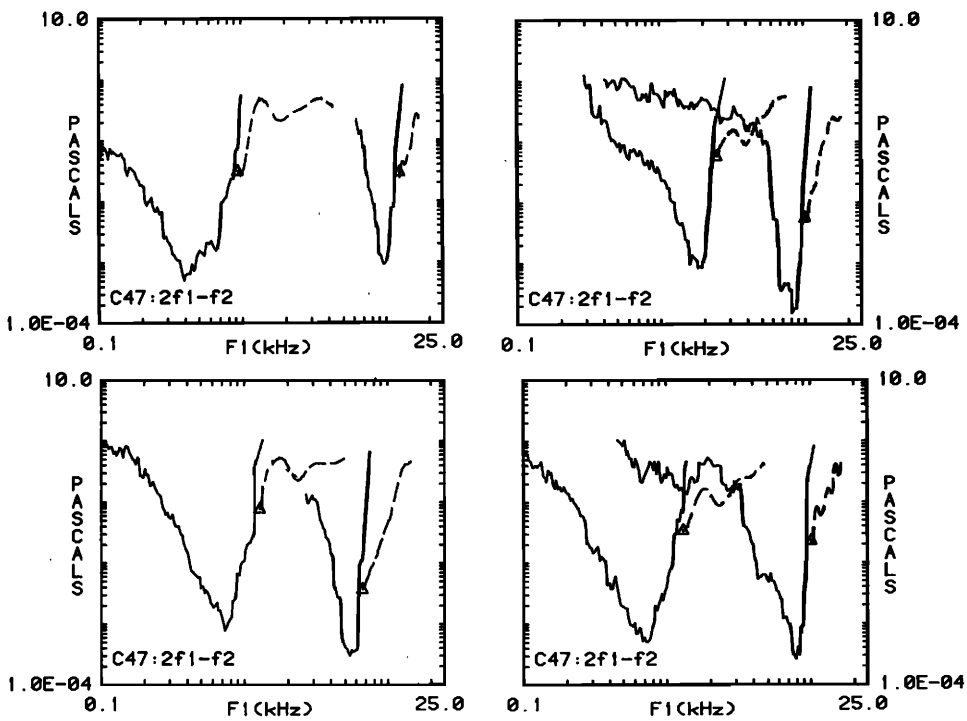

FIG. 2. For cat 47 the spline fit DTC (dashed curve) is plotted with the FTC for eight units. The spline fit was used to provide a least squares average for multiple DTC runs. The distortion product is $2f_1 - f_2$.

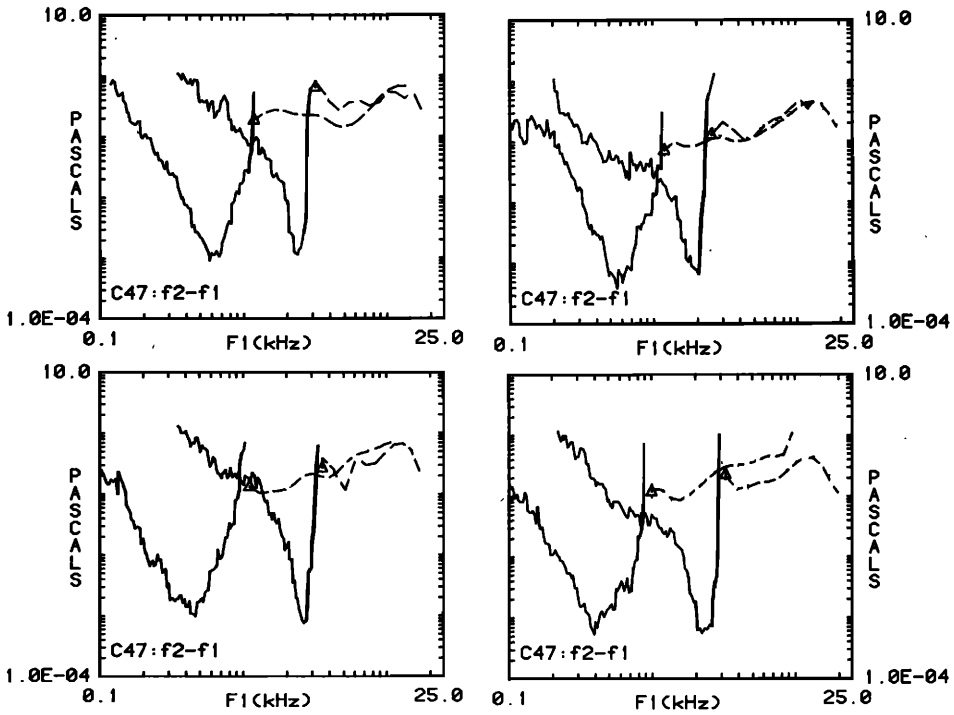

FIG. 3. Same as Fig. 2 except the distortion product is $f_2 - f_1$. The dashed curves are the $f_2 - f_1$ DTCs while the solid curves are the FTCs.

every animal that we have studied, changing the gain by x dB usually results in an increase of at least x dB in the DTC and not in an increase of $x/3$ dB as one would expect from a purely cubic nonlinearity. Shown in Fig. 4(e) are DTCs measured with three different ratios of A_1 to A_2. One set of DTCs is measured in the usual way with $A_1 = A_2$; one is measured with $A_1 = 3A_2$; and the third is measured with $A_2 = 3A_1$. The superposition of these cases suggests that the nonlinearity is not of the form $A_2 A_1^2$. The observation of Fig. 4(e) has been found in all animals. The DTC is independent of the ratio of A_1/A_2 until that ratio becomes greater than 4 or 5 or less than 0.2 or 0.25.

Besides normalization by detector threshold, we found that the transformation of the frequency axis from $\log f_1$ to $\log(f_2/f_1)$ generally unifies the $2f_1 - f_2$ data across frequencies. In Fig. 5, we see the results of this transformation. Figure 5(a) is the complete set of RDTCs for one animal; in Fig. 5(b) these RDTCs are replotted with abscissa $\log(f_2/f_1)$. Figure 5(c) and (d) shows the same for another animal. For frequencies of $2f_1 - f_2$ above 3 kHz, we found that both the normalization by detector threshold and rescaling the frequency axis to $\log(f_2/f_1)$ were most effective in unifying the data. These transformations were unifying in four of the five animals for which we had extensive data across many frequencies.

In Figs. 1, 2, 4, and 5 it is apparent that nonmonotonic features of the DTCs are commonplace. Furthermore, it is generally evident that at high CFs the detectable distortion

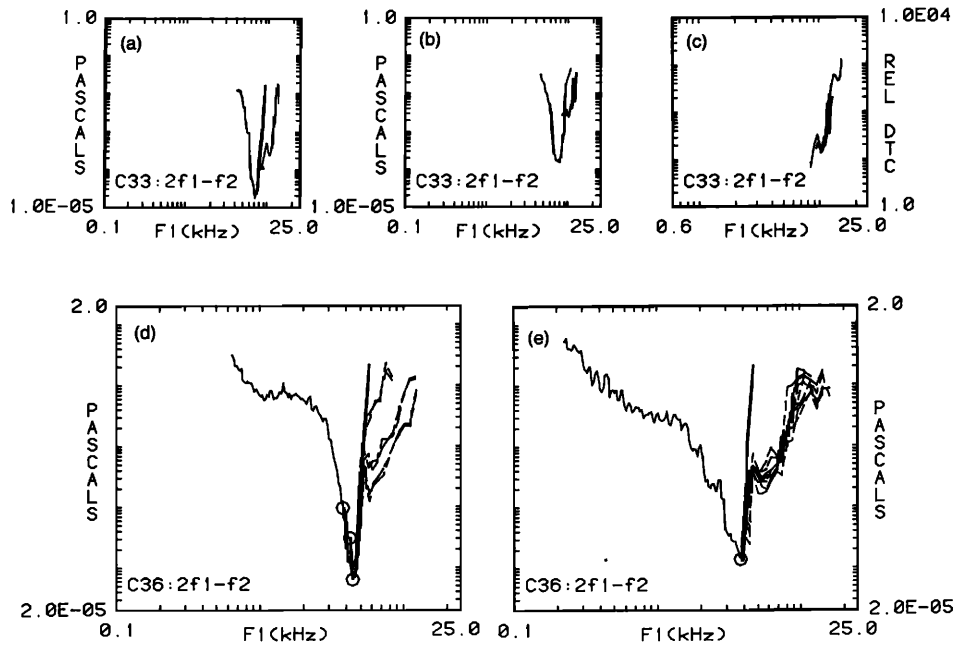

FIG. 4. (a) and (b) shows two FTCs with the respective DTCs. (c) Shows the DTCs normalized with respect to the FTC at CF. Notice that the normalization superimposes the DTCs. (d) Shows three pairs of DTCs; one detected when the $2f_1$–f_2 DP's frequency equaled the CF frequency—hence, the amplitude of the DP equaled the FTC at CF; and the other two detected when the $2f_1 - f_2$ DP's frequency was less than CF (as shown by the circles)—hence, the amplitude of the DP was equal to the value of the FTC at these frequencies. Notice that a 20-dB change in DP amplitude is associated with a 20-dB change in the level of the DTC. (e) Shows three sets of DTCs. The first detected when $A_1 = A_2$; the second detected when $A_1 = 3A_2$; and the third detected when $A_2 = 3A_1$. Notice that the three DTCs are essentially the same.

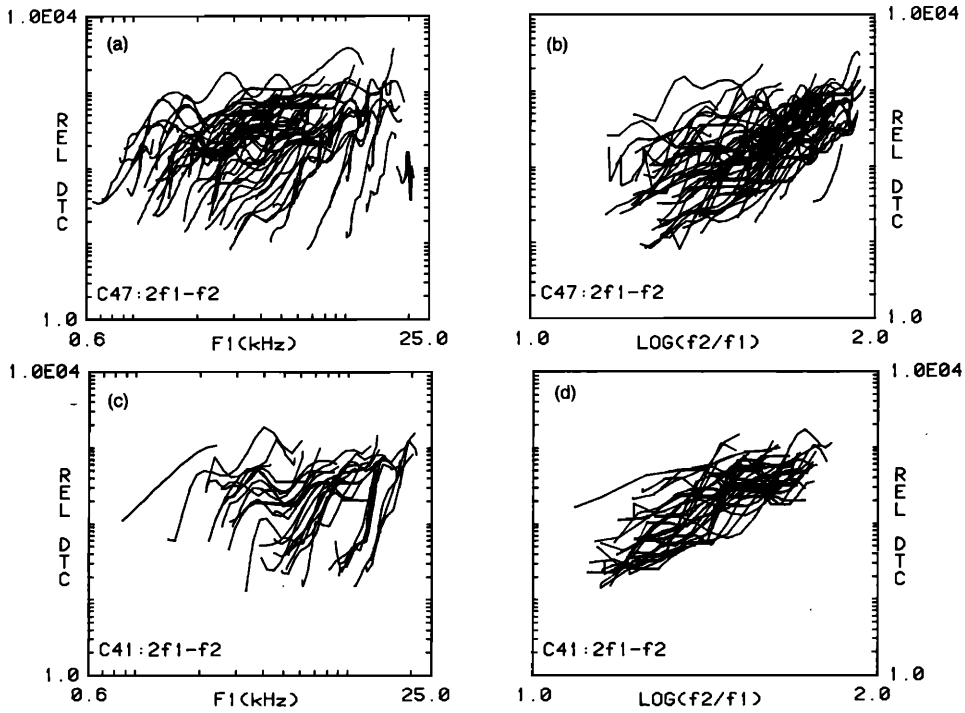

FIG. 5. (a) We show here a collection of plots of the cubic spline fits to the $2f_1 - f_2$ RDTCs of cat 47. The density of curves is too great to resolve the individual curves but the trends in the RDTCs with frequency are apparent. (b) The $2f_1 - f_2$ RDTCs are plotted versus f_2/f_1 on a logarithmic scale. Disregarding nonmonotonicities, generally the RDTCs approximate straight lines of the same slope independent of the CF of the unit. (c) and (d) This plot is the same as (a) and (b) for a different animal.

products can be generated at lower amplitudes (relative to the CF threshold) of the primaries. The data generated for and after cat 36 were taken using a Kaiser windowed two-tone complex of 50-ms duration (Kaiser, 1966). Data taken prior to cat 36 used a cosine windowed (Hanning window) tone pip of 50 ms. Since the Kaiser windowed tone pip had 20 dB smaller sidelobes than the Hanning window, it was used to convince us that the signal driving the unit was not due to the sidelobes of the f_1 primary tone as f_1 approached the CF. Generally, we found that the RDTC generated with the Kaiser windowing was about 6 dB higher (i.e., less detectable) than with the cosine windowing as f_1 approached CF. However, both the Kaiser driven and Hanning driven RDTCs showed the same general features.

As is seen in Fig. 5, if the RDTC data are replotted versus $\log f_2/f_1$, the average slopes are generally found to range from 40–70 dB/oct (of f_2/f_1) with a mean across animals of about 55 dB/oct (of f_2/f_1). From the Liberman (1982) cochlear map, 1 oct of f_2/f_1 corresponds to 3.6 mm of distance along the basilar membrane. The intercepts of these curves are 10–20 dB above the FTC at CF, which represents an estimated DTC at $f_{CF} = f_1 = f_2$.

In Fig. 6 we show a plot of the dependence of several $f_2 - f_1$ RDTCs upon frequency for cat 47. For the case of $f_2 - f_1$, f_1 seems to be the most appropriate independent variable. As before, the frequency of the DP equals the CF of the unit under study and the amplitude of the DP is held equal to the threshold response at CF. All responses have been normalized by the CF threshold. It seems clear from Figs. 6 and 3 that, at least for higher CFs, the $f_2 - f_1$ RDTC is much less frequency dependent than the $2f_1 - f_2$ RDTC (Figs. 1, 2, and 5). Also, we found a much larger variability between cats for the $f_2 - f_1$ DP, whereas all of our cats with good thresholds showed a fairly similar threshold normalized $2f_1 - f_2$ DP.

B. Ear canal acoustic distortion products

In Fig. 7 we show FTCs from two different cats along with the amplitudes of the f_1 and $2f_1 - f_2$ Fourier components of the ear canal pressure. The Fourier component of the ear canal pressure at frequency f_1 is symbolized by the line labeled by a □. The curve labeled by the ⅄ represents the ear canal pressure Fourier component at the distortion product frequency $2f_1 - f_2$ *and it is also plotted as a function of* f_1. In Fig. 7(a) and (b), the Fourier components were measured using the Kiang–Moxon paradigm to hold the neural DP at threshold. We shall refer to this as the "closed-loop" condition. Note that the f_1 pressure Fourier component follows the DTC trajectory, while the $2f_1 - f_2$ Fourier component remains approximately constant at the threshold of the FTC at CF (at $2f_1 - f_2$). In Fig. 7(c) and (d), the ear canal pressure has been measured with full output to the acoustic driver ("open-loop" condition). In this case, the f_1 Fourier component follows the "cavity" response of the animal's

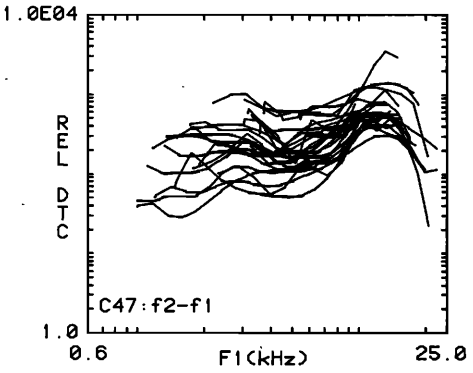

FIG. 6. Plot of the cubic spline fits for the $f_2 - f_1$ DTCs of cat 47. It is quite evident here that the frequency dependence of the $f_2 - f_1$ DP differs from that of the $2f_1 - f_2$ DP.

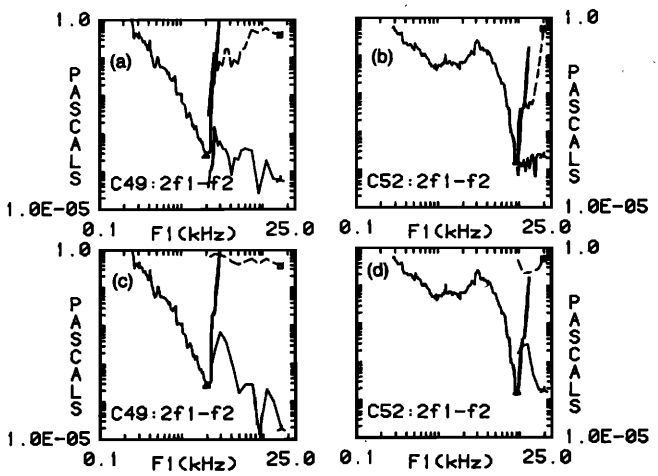

FIG. 7. (a)–(d) shows FTCs (solid lines) from two different animals along with the amplitude of the ear canal pressure at f_1 (short dashes) and the amplitude at $f = 2f_1 - f_2$ (longer dashes) as a function f_1. In (a) and (b) the DTC paradigm is enabled; hence, the f_1 amplitude follows the DTC trajectory while the $2f_1 - f_2$ amplitude remains near the threshold of the FTC at CF. In (c) and (d) the DTC paradigm is disabled and the f_1 component follows the ear acoustic cavity response while the ear canal DP $2f_1$–f_2 increases as f_1 approaches f_{CF}. Note that the $2f_1 - f_2$ amplitude trajectories in (c) and (d) approximately mirror the f_1 amplitude trajectories in (a) and (b). Notice that when the distortion product generation is largest, the difference between the level of the f_1 primary and the level of the distortion product is about 30–40 dB in (a), (b), (c), and (d) (namely, all cases).

outer and middle ear system while the $2f_1 - f_2$ pressure Fourier component increases in magnitude as f_2 approaches f_1. Notice that the $2f_1 - f_2$ Fourier component curve in Fig. 7(c) and (d) is, roughly speaking, a "mirror" image of the f_1 Fourier component (the DTC) in 7(a) and (b). This might be expected if one assumes that the level dependence of the DPs is less marked than the dependence on relative frequency.

Our interpretation of Fig. 7 (and of similar data acquired from other animals) is that the level of the distortion product as measured in the ear canal, when held at the neural threshold, is sufficient to drive the unit directly. It was initially surprising to us that the DP would be this high. Of course, by definition of the closed-loop condition, it could not be higher than the threshold at CF or the measurement would be inconsistent; but, it could have been lower. Essentially, the ear and our sound delivery system form a closed system and the DP, which is most likely generated in the cochlea, exists at a high enough level that its value in the ear canal is sufficient to drive the neural unit under study. It follows from this study that it is not necessary to measure the DPs neurally; they could be determined more accurately, faster, and as a function of level, by ear canal measurements alone.

III. DISCUSSION

Our observations of the levels of the $2f_1 - f_2$ DP and the nonmonotonicity of $2f_1 - f_2$ DP are in agreement with the observations of Buunen and Rhode (1978) in the auditory nerve of the cat. Also their observations that the strength of DP generation is greater for high distortion frequencies (CF > 5 kHz) is corroborated by our Fig. 5(a) and (c) (and by similar data from several other cats). We have extended their results by our more extensive frequency-dependent iso-DP threshold data. Moreover, for the first time, we have compared the $2f_1 - f_2$ DPs seen at the level of the auditory nerve with cochlear generated $2f_1 - f_2$ DPs measured acoustically in the ear canal. We have also shown a linear relation (Fig. 4) between the DP threshold and the CF threshold. These indicate that DP threshold, when normalized by the CF threshold, is approximately independent of the unit threshold.

In Fig. 8, in the left column, we show DPT points (i.e., the points of intersection of the DTC with the FTC) plotted as a function of threshold of the FTC at CF (i.e., the value of the amplitude of the distortion product). Generally, but not always, the DPT corresponded to the lowest value of the primary amplitude A that generated a detectable distortion product. In the right column, the DPT normalized by the threshold is plotted. Notice that the normalization takes away the dependence of DPT on threshold. Indeed, there is much scatter in the data for reasons that are not at all clear to us. It also might be noted that the correlation of the DPT with CF threshold seen with cats 33, 35, and 41 was not at all as clear with cats 36 and 47. As others have observed (e.g., Buunen and Rhode, 1978), we find here that A_D/A_{CF} is approximately constant. Improved information on this level dependence question would be more easily answered by making measurements in the ear canal as a function of level (which we have not done yet).

We also find good agreement with the studies of distortion products in the anteroventral cochlear nucleus (AVCN) of the cat as found by Buunen *et al.* (1977) and Smoorenburg *et al.* (1976). Smoorenburg *et al.* (1976) showed, as do we, that the generation of $2f_1 - f_2$ DP is much more frequency dependent than the generation of the $f_2 - f_1$ DP. Moreover, the nonmonotonicities in $2f_1 - f_2$ that we see in the auditory nerve are also seen in the AVCN studies. This may not be surprising, since many neurons in the AVCN show level and frequency responses that are quite similar to the neurons of the auditory nerve.

The levels of DPs in the external auditory meatus that we observed are consistent with what has been observed by others (Kim *et al.*, 1980; Siegel and Kim, 1982; Mountain, 1980; Zurek *et al.*, 1982). Distortion products 40 dB below the primaries (thresholds 40 dB above) are easily and routinely detectable. Most importantly, for stimulus levels corresponding to neural DP thresholds, the $2f_1 - f_2$ DP measured in the ear canal is similar to the unit's CF threshold (Fig. 7). Since it is easier and more accurate to measure the distortion products in the ear directly, it follows that we might avoid the many problems and complexities of neural DP measurements by making the equivalent acoustic ear canal DP measurements.

To understand why the transformation of the DTC to a $\log(f_2/f_1)$ frequency axis would be expected to unify the data (assuming that the distortion product is generated in the cochlea), consider the following heuristic model. Idealize the basilar membrane (BM) response to have triangular shape (Rhode, 1978; Zwicker, 1981), where the basal slope m is of lower absolute value than the apical slope, as shown in Fig. 9. Since the characteristic place corresponding to frequency f is proportional to $\log f$, the idealized BM response can be de-

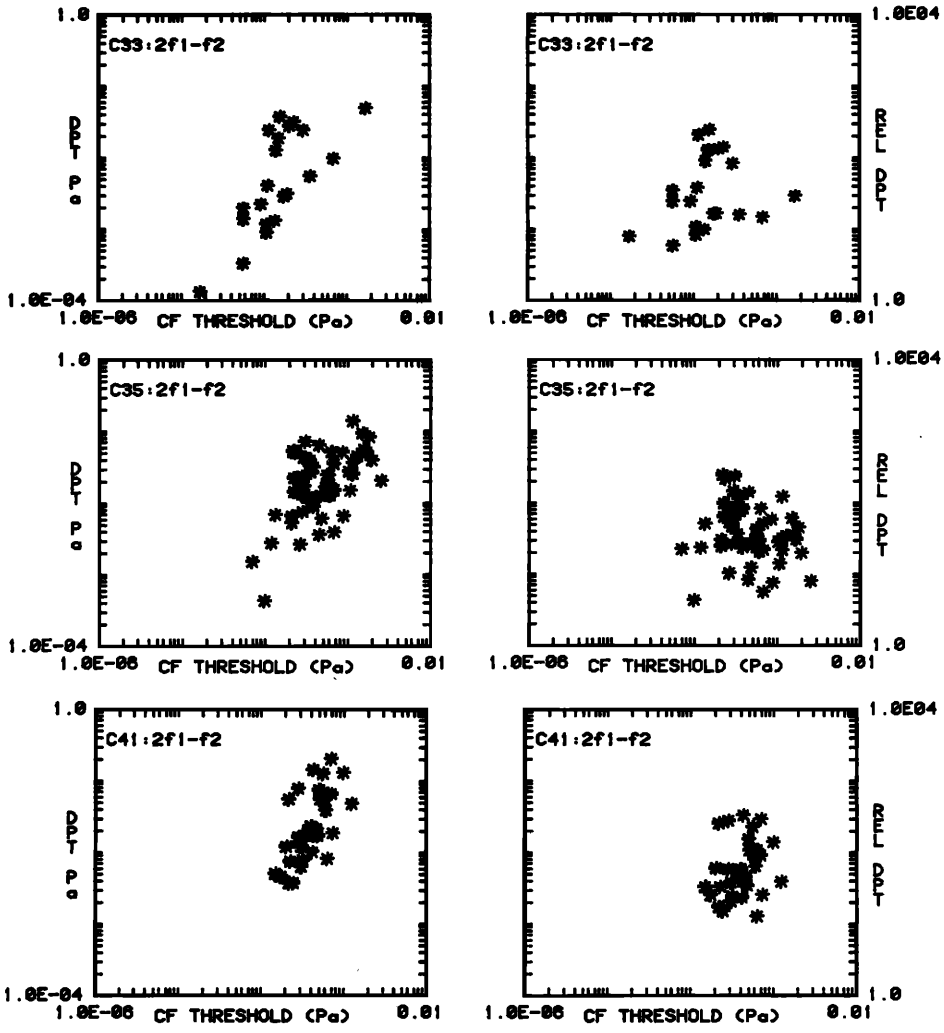

FIG. 8. Left-hand column is a plot of the DPT points (points of intersection of the FTC with the DTC) versus CF threshold. The right-hand column shows the DPTs normalized by the CF threshold. Notice that the normalization seems to remove the correlation of DPT with CF threshold.

scribed on the low-frequency side (and also on the high-frequency side) by log (response) being proportional to log (frequency). We assume that the BM response is quasilinear, to a first approximation, in that the response to a two-tone input is the superposition of the responses of the individual tones.

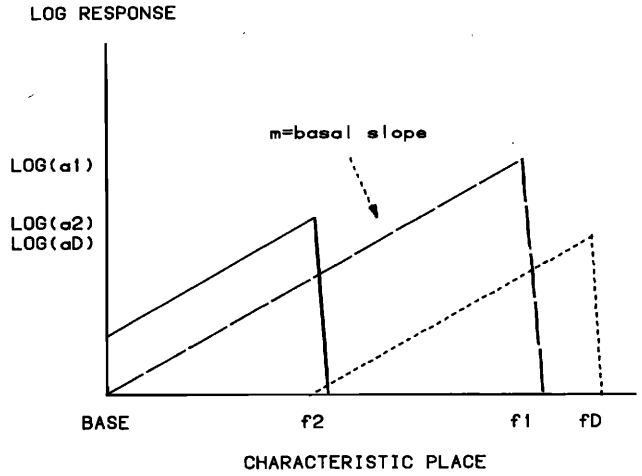

FIG. 9. Basilar membrane displacement is idealized to have the illustrated triangular shape when the logarithm of response is plotted versus distance along the basilar membrane. Shown are the responses to a tone of frequency f_2 (solid line), to a tone of frequency f_1 (long dashes), and to a tone of distortion product frequency f_D (short dashes).

Also, assume that the distortion product generator can be described by a power law nonlinearity and that the distortion product is generated at the f_2 place. In particular, consider the $2f_1 - f_2$ distortion product and assume that it is generated by a cubic nonlinearity of the form $a'_D = \alpha a_2 (a'_1)^2$; where a'_D is the amplitude of the BM displacement at the distortion product frequency f_D at the f_2 place, α is the frequency-dependent strength of the distortion product generator, a'_1 is the amplitude of the BM displacement due to a tone of frequency f_1 at the f_2 place, and a_2 is the amplitude of the BM displacement due to a tone of frequency f_2 at the f_2 place. The primed quantities refer to responses at the f_2 place of frequencies not equal to f_2. [The generalization to other distortion products and other orders of nonlinearity is straightforward (Weiner and Spina, 1980) and will not be considered here.] From Fig. 9 it is evident that, due to the constant slope m on the basal side of the response curves,

$$\log a'_1 = \log a_1 - m \log(f_2/f_1), \tag{1}$$

$$\log a'_D = \log a_D - m \log(f_2/f_D), \tag{2}$$

where a_D is the amplitude of the distortion product at its characteristic place. Now, using (1) and (2) and the relationship $a'_D = \alpha a_2 (a'_1)^2$, we have

$$\log a_D = \log \alpha + \log a_2 + 2 \log a_1 - 2m \log(f_2/f_1) + m \log(f_2/f_D). \tag{3}$$

Assuming again quasilinearity, the BM displacement (a_1 or a_2) will be proportional to the input pressure amplitude (A_1 or A_2). Also, to be consistent with most of our data, let $A_1 = A_2 = A$. Therefore,

$$\log A_D = \log \alpha + 3 \log A - 2m \log(f_2/f_1) + m \log(f_2/f_D), \quad (4)$$

where A_D is the pressure that is proportional to a_D and α has beeen redefined to include the proportionality between pressure and basilar membrane displacement. In the DTC paradigm, a_D is held constant; so the DTCs would be described by

$$\log A = 2/3m \log(f_2/f_1) + 1/3 \log(A_D/\alpha) - (m/3) \log(f_2/f_D). \quad (5)$$

Equation (5) can be simplified further if one makes the assumption the α is not a constant but that it depends on the linear dynamical response of the BM at the f_2 place to a signal of frequency f_D; i.e., let α assume the same frequency dependence as described in Fig. 9 and as implemented in Eqs. (1) and (2),

$$\log \alpha = \log \delta - m \log(f_2/f_D), \quad (6)$$

where δ is a frequency-independent measure of the generator strength. This assumption is mathematically equivalent to the "weighting" function in Goldstein's (1966) discussion of the psychophysical properties of the cubic distortion product.

Substituting (6) and (5) leads to the description of the DTC as

$$\log A = 2/3m \log(f_2/f_1) + 1/3 \log(A_D/\delta). \quad (7)$$

That is, the slope of the DTC or the RDTC plotted versus $\log(f_2/f_1)$ will equal 2/3 of the slope of the BM membrane excitation. From Fig. 5, $2/3m$ is approximately 40–70 dB/oct; thus m is between 60–105 dB/oct. An m of 60–150 dB/oct corresponds to the slope range of the neural tuning curves below their CF (Allen, 1983). This correlation of the DTC slope with the FTC slope below CF argues in favor of cochlear generated $2f_1 - f_2$ DPs (Smoorenburg *et al.*, 1976; Zwicker, 1981). Also, notice that if $\Delta(\log A_D)$ is required to equal $\Delta(\log A)$, as the data show, then δ is proportional to $A_D^{-\gamma}$ where γ equals 2. Necessarily, the assumption of the power law nonlinearity is insufficient to describe the data as a function of level.

Using the same model to describe the $f_2 - f_1$ DTCs, one finds that the slope of the DTC versus $\log(f_2/f_1)$ is $m/2$ when a second-order nonlinearity is assumed and that the slope is $m/4$ when a fourth-order nonlinearity is assumed. From Fig. 7 it is apparent that the $f_2 - f_1$ DTC slope is much less than the $2f_1 - f_2$ DTC slope. Indeed, the slope of $f_2 - f_1$ is better approximated by the fourth order nonlinearity than a second order nonlinearity.

The electrical analog model of Hall (1981), which uses a resistive element of the form

$$R_i = R_{i0}(1 + \gamma I_i^2), \quad I_i > 0,$$
$$R_i = R_{i0}, \quad I_i < 0, \quad (8)$$

where R_i is the resistance of the ith section of the model and I_i is the current through the ith section, is also capable of generating $f_2 - f_1$ DPs that are less dependent upon relative frequency than the $2f_1 - f_2$ DPs (Hall, 1974, and our Figs. 5 and 6). Hall's model suggests that the nonmonotonic behavior is due to the interference of the direct DP wave with a wave propagated toward the stapes which is partially reflected back.

An alternative explanation of the nonmonotonicities which was suggested by Zwicker (1981) is also supported by some of our data as well as by the data of Kim *et al.* (1980). Zwicker has described the nonmonotonicities in terms of a level dependent superposition, at the distortion product place, of wavelets generated by the basilar membrane in the vicinity of the f_1 and f_2 places. We have taken data [Fig. 4(d)] where we have changed the gain of the detector by setting the DP frequency away from CF. For sharply tuned units this can change the gain by 10 dB while only changing the DP frequency by a factor of 0.9. Frequently, this smooths out nonmonotonic behavior in the DTC. At this time, we do not have enough systematic data to rule out one explanation of the nonmonotonicities in favor of the other.

IV. CONCLUSION

We have found that in a sealed ear canal, when corrected for loading by the impedance of the source, the magnitude of the acoustic $2f_1 - f_2$ DP appears to be sufficient to account for threshold levels of neurally measured DPs. This result is one of the more surprising conclusions of this study. Since we have ruled out distortion product generation by the acoustic delivery system, it appears that there are two possibilities for the source of these distortion products. First, the distortion product could be generated within the middle ear structure. Second, the distortion could be generated within the cochlea and could propagate backward (via the middle ear) into the external auditory meatus. Given the strong frequency dependence of $2f_1$–f_2 DP generation and given that a plot of the DTC versus $\log(f_2/f_1)$ seems to be more tightly clustered over the frequency range than DTC versus f_1, it appears that the cochlea is a more likely source of the $2f_1$–f_2 DP than the middle ear. The concept of a wave propagated toward the stapes (Hall, 1981) and partially coupled into the middle ear seems consistent with our observation of substantial distortion product levels in the ear canal. Matthews (1983) has investigated this model using numerical methods.

V. TWO-TONE SUPPRESSION

A. Methods

We also used a modified version of the Kiang–Moxon paradigm to measure two-tone neural rate suppression. In this second study of cochlear nonlinearities we measured the FTCs of units along with rate suppression threshold curves (STC). The rate suppression threshold curve was defined in the following way.

During one 50-ms interval we present a single suppressor tone at the suppressor frequency f_s. During the adjacent 50-ms interval, we simultaneously presented two tones; one which we term the excitor was usually at a level of between 6–10 dB above the FTC at CF (these CF tones are symbolized by the triangles or squares in Fig. 10), while the second simultaneous tone was a repeat of the suppressor tone. The

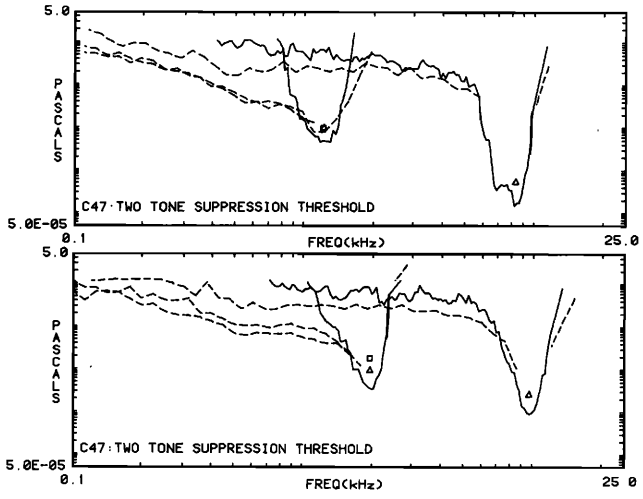

FIG. 10. In this figure we show FTCs (solid curves) along with the threshold of suppression curves (dashed lines). The tone that is being suppressed (the excitor tone) is marked by a triangle or square. For one unit (CF = 2 kHz) there are two excitor tones that differ in level. The higher suppression threshold curve corresponds to the larger CF excitor tone.

level of the suppressor tone was varied systematically until the number of spikes generated during the single-tone 50-ms interval was *one less* than the number of spikes generated during the two-tone 50-ms interval. As seen in Fig. 10 the trajectory of the levels of the suppressor tones found in this way in frequency-amplitude space (dashed lines) is defined as the suppression threshold curve (STC). The implementation of the "threshold" paradigm is presented graphically in Fig. 11. In this figure, the upper panel shows an abstracted FTC with an excitor tone (symbolized by the triangle) at a frequency equal to the CF having an amplitude A_{CF}. At a frequency equal to f_s we would like to find the amplitude A_s of a suppressor tone as previously described. In the middle panel, we show two abstracted rate-level functions due to the suppression tone alone (at frequency f_s) and the suppression tone plus the excitor tone together. *This panel further shows that for the two-tone input situation, over part of the range of the rate-level function, the level can be a double valued function of rate.* If the level as a function of the rate is not single valued, then a threshold value is not uniquely defined, and unstable conditions can result, such as the results of Schmiedt (1982) which are ill defined at low frequencies. However, the difference between the rate-level function with and without the excitor tone has a single valued inverse. This difference is shown in the bottom panel. Since we would like our suppression threshold curve to be based upon a well-defined quantity, we implemented the modified Kiang–Moxon paradigm to find the level of the excitor tone where the difference in the rate-level curves equaled one spike per 50 ms. The level of the excitor tone found in this way is shown in the bottom panel of Fig. 11 as A_{TH}.

A simple physical interpretation of the threshold defined by this procedure is as follows. When the STC lies below the FTC, then the suppressor was successful in reducing the driven rate (due to the CF excitor tone) to one spike more than the spontaneous rate R_s. When, on the other hand, the suppression threshold A_{TH} is greater than the FTC threshold, then the suppressor was unsuccessful in reducing the rate to the spontaneous rate. (It is generally accepted that a suppressor cannot reduce the spontaneous rate.) A major advantage of defining the suppression threshold in the way that we have is that both the FTCs and the STCs are always measured at the same point on the rate-level curves for the individual units; i.e., FTCs and STCs are measured as the average rate just begins to increase with level above the spontaneous level. Physically, our suppression thresholds comprise the locus of points in frequency-level space that make a probe tone ineffective (as far as an average rate is concerned).

B. Results

In Fig. 10 we show suppression thresholds for four different units. The symbols △ and □ show the placement of

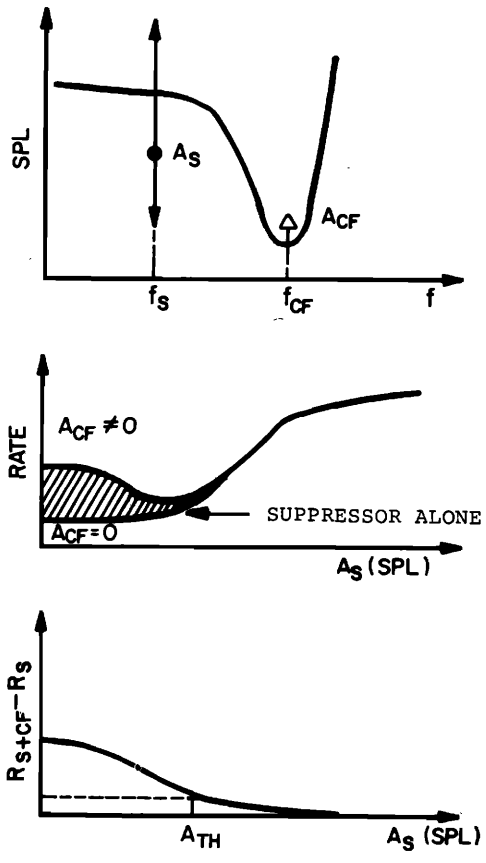

FIG. 11. The upper panel of this figure shows a hypothetical unit's FTC along with an excitor tone at CF of amplitude A_{CF}, and line at frequency equal to f_s, where we scan, in amplitude, a probe tone of amplitude A_s. Along this locus of amplitudes a value of A_s can exist such that the response to A_{CF} is reduced to its spontaneous rate. This value of the suppression is defined as the threshold A_{TH}. In order to understand how the threshold of suppression is defined, the middle and the bottom panels of this figure are useful. In the middle panel, the spike rate due to the probe tone both with and without the CF excitor tone is pictured. The hatched region is the difference between the two spike rates. The difference is plotted in the bottom panel. Notice that the rate difference is a monotonic function of level whereas the rate itself (in the middle panel when $A_{CF} \neq 0$) is nonmonotonic. As is explained in the text, this is one reason why the rate difference, rather than a rate increment, was used in the suppression threshold measure. Further, the suppression threshold defined in this way is measured at the same point on the rate-level curve as the FTC is measured (i.e., 1 spike per 50 ms above spontaneous).

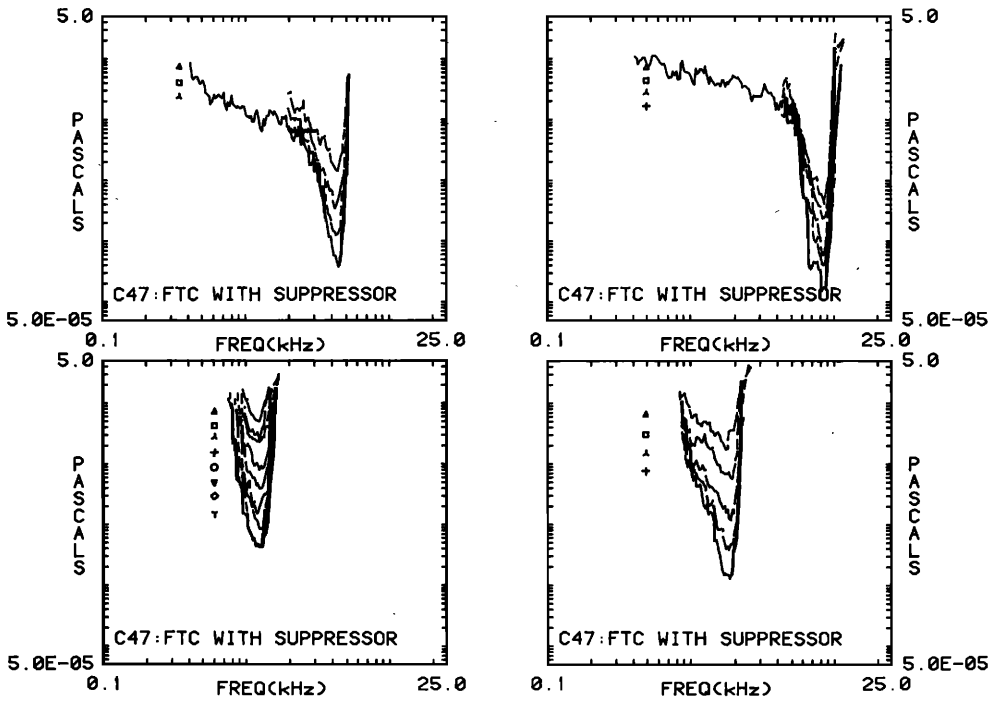

FIG. 12. We show here FTCs for four units. The FTCs were remeasured in the presence of a second (suppressor) tone with the frequency and amplitudes of the suppressors as indicated by the symbols. The higher the level of the suppressor tone the corresponding higher the level of the tip of the threshold tuning curve.

the excitor tone, while the dashed line shows the locus of A_{TH} as defined above. As explained, for suppressors above the dashed line, but below the FTC threshold, the unit fires at less than the spontaneous rate plus one spike per 50-ms interval.

Besides having the advantage of being a measure of a single valued (well defined) quantity, our measure of suppression threshold is consistent with an alternative measure of two-tone suppresssion as shown in Fig. 12.

In Fig. 12 the FTC (near CF) is remeasured (using the Kiang–Moxon paradigm) in the presence of a subthreshold suppressor tone. The levels and frequencies of the suppressor tones are symbolized by the geometric symbols (□, +, △, etc.) and the "suppressed" FTCs are the curves nested above the FTC. The larger the suppressor, the larger the corresponding FTC threshold curve.

One unit pictured in Fig. 10 ($f_{CF} \approx 2$ kHz) shows two suppression threshold curves and two different excitor tones (△,□). From this unit and from all the data in Fig. 12, we see that for excitor tones near the CF, the neural excitatory threshold increases as the subthreshold suppressor increases. From Fig. 12 it appears that for excitatory tones at CF, an increase of 6 dB in suppressor tone level results in a 10- to 12-dB increase in the suppression threshold. This seems to be true over a fairly large suppressor level range—as long as the suppressor is neither so low as to be below the STC threshold nor so high as to be above the FTC threshold. Note that two of the units in Fig. 12 show CF suppression over a 40-dB range. For excitor frequencies away from the CF, the suppression effect is much less. Such large (40 dB) rate suppression effects are only seen in sharply tuned units.

In Fig. 13 one can see the general features of the frequency dependence of the STC. The STCs of Fig. 10 and Fig. 13 are fairly level independent over a broad frequency range for high CF units. The most striking aspect of Fig. 13 is the constant value for the STCs for the higher frequency units (CF greater than 2 kHz). This behavior is also apparent from Fig. 10 and suggests that there is a master curve that defines suppression by tones below the CF tone. These thresholds generally range between 60 and 80 dB (*re*: 20 μPa) in level. Moreover, for units where we have measured the low-frequency tails of the FTC, the suppression threshold parallels the low-frequency tail.

C. Discussion

Thus we have found that the threshold for CF excitor two-tone rate suppression follows the middle ear response

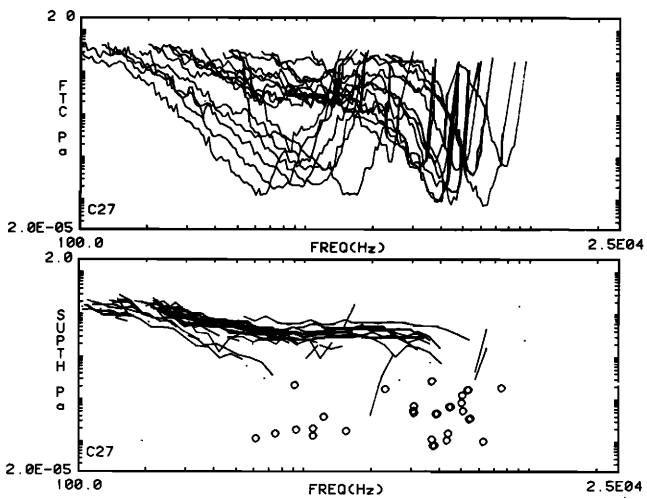

FIG. 13. In this figure we show many superimposed STCs (lower) and FTCs (upper) from animal 27. Notice that, as in Fig. 10, the STCs are fairly constant in frequency over a broad range (0.5 kHz $< f <$ 5 kHz). Above CF the STC is sharply frequency dependent and almost parallels the high-frequency side of the FTC. The open circles represent the excitor frequencies just above (or, sometimes, at) the CF thresholds.

(as does the tuning curve tail response, Nedzelnitsky, 1974). This result was also found by Schmiedt (1982) using a different threshold criterion and was reported by Allen (1981).

One can also note from Fig. 10 that there is negligible suppression (as defined here) at frequencies above CF. We found this to be generally true in that the amount of suppression observed above CF was much less (or was absent) relative to that seen below CF. For most units having CFs below 1 kHz with low thresholds (namely, most low-frequency units) no rate suppression effect was observed either above or below CF.

The rate suppression effect is largest for low spontaneous units having high thresholds. Because the low spontaneous units usually have higher relative thresholds, these units show a larger relative two-tone suppression since the suppression threshold seems to be almost independent of the unit's CF threshold. When most of the FTC is above 80 dB SPL, the response at CF can be more easily suppressed. A unit of this type may be seen in Fig. 10, upper panel, 1200-Hz CF unit.

We define the suppression threshold, as a function of the suppression frequency, to be any suppressor level that reduces the response [due to the (CF) excitor tone] to one spike more than the spontaneous rate. Families of suppression thresholds may be generated (as in Fig. 10) which correspond to the different excitor amplitudes at CF. Alternatively, we may measure FTC curves (as in Fig. 12) made in the presence of a subthreshold suppressor tone. As such, the suppression threshold, as we have defined it, has a nice interpretation in terms of the suppressed FTC response curves made in the presence of a suppressor tone. Suppose that a particular A_{CF} of Fig. 11 produces an STC threshold A_{TH} at frequency f_s. When that value of A_{TH} is used in a suppressed FTC experiment (as in Fig. 12), then the resulting FTC will pass through the original A_{CF} of the first experiment. In other words, one set of curves is consistent with the other

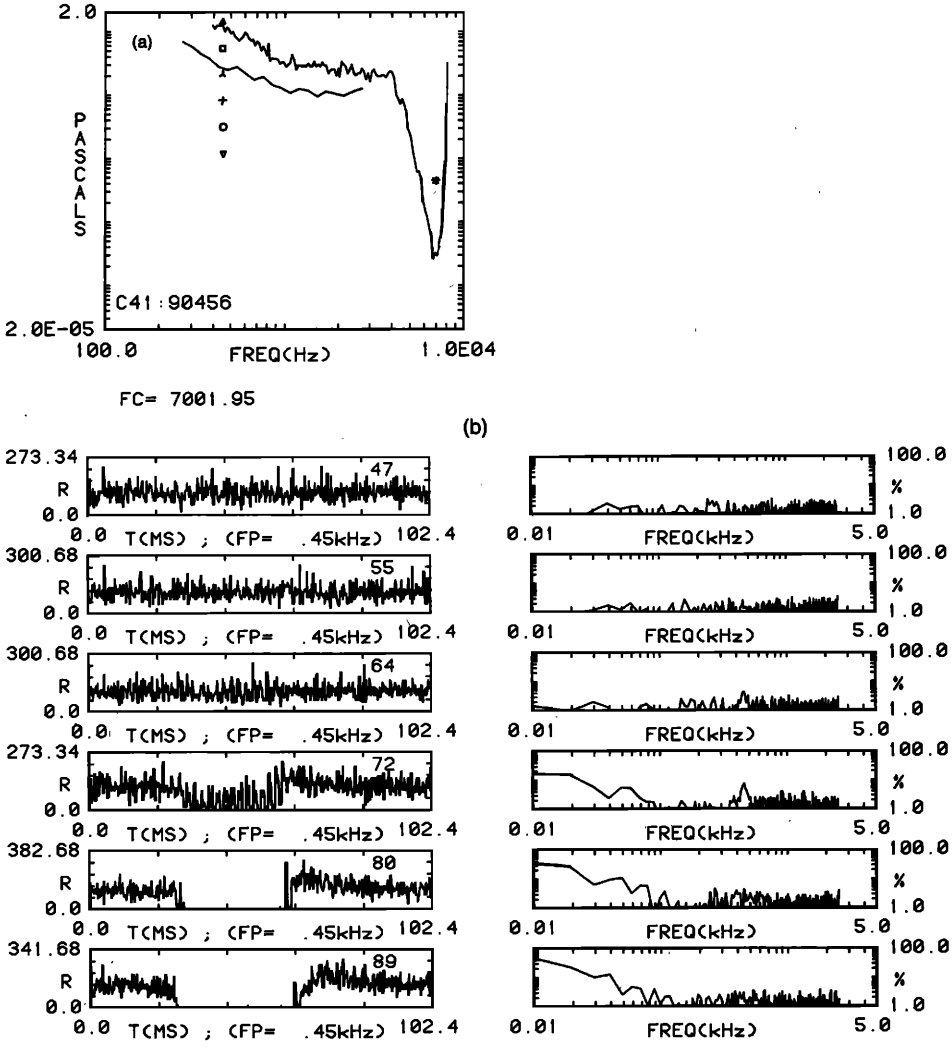

FIG. 14. (a) The FTC and the STC for a unit along with the frequencies and levels of a series of suppressor tone pips (geometric symbols) are shown. A continuous excitor tone (the asterisk) at the CF frequency was input to test suppression by the tone pips. (b) The series of post-stimulus time histograms measured during the input of the suppressor tone pips in the presence of the continuous CF tone are in the left column and the Fourier transforms (expressed as synchrony) of the histograms are in the right column. FC is the frequency of the CF tone. The frequency of the suppressor is written under each histogram. The level of the suppressor, in approximate dB SPL, is written in each histogram box. The synchrony plotted in the right column is plotted on a log percentage scale. Note that the unit is synchronized to the suppressor tone only over a very limited range of level, and is never driven by the suppressor.

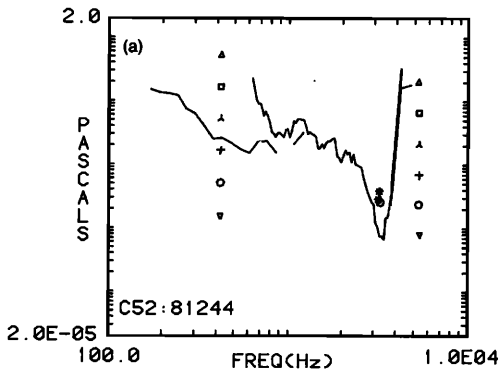

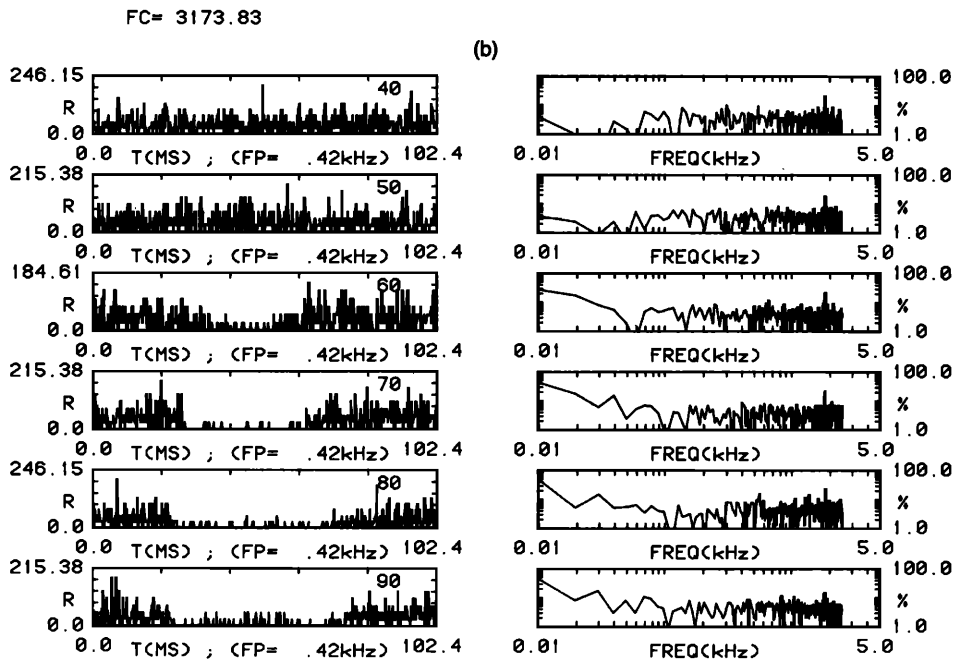

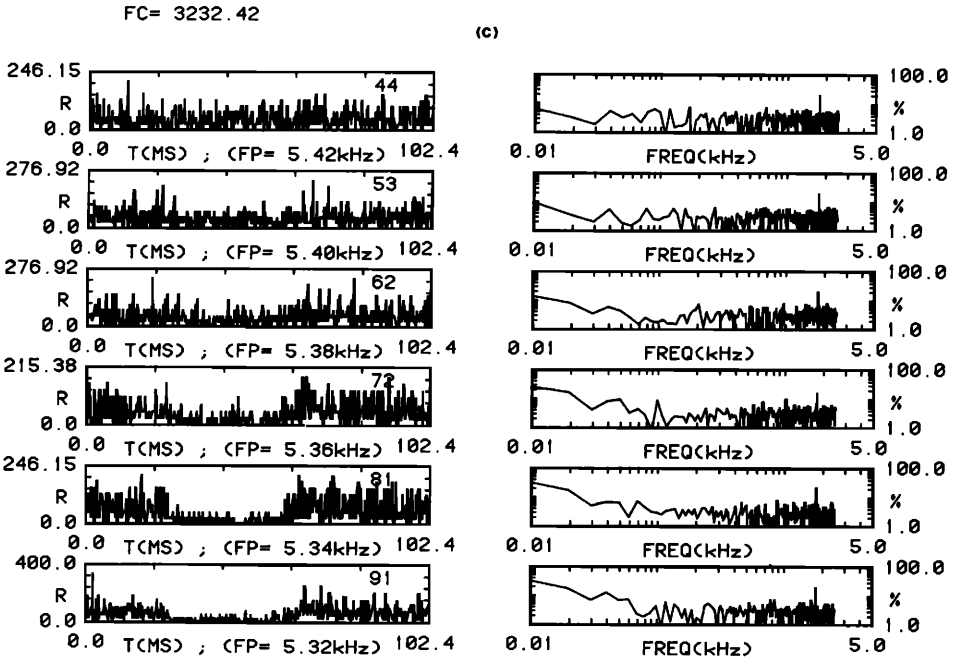

FIG. 15. (a) FTC and STC for a 3.4-kHz unit. The geometric symbols show the probe suppressor levels above and below CF at 420 Hz and 5.42 kHz. (b) Histograms and synchrony below CF. (c) Histograms and synchrony above CF. The asterisks mark the tones at CF.

when, and only when, one defines the measures as we have here.

Another finding, for the majority of our units, was that the suppression effect above CF was not as strong as that below CF. Indeed, only for units with high threshold at CF did we find measurable suppression by a tone above CF. Abbas and Sachs (1976) found substantial suppression above CF using a fractional rate response measure. Their data indicate that the units showing these suppression effects generally had thresholds at CF of 40 dB SPL and greater (see Figs. 1–4 of Abbas and Sachs, 1976). Hence, their results showing substantial suppression above CF do not seem to be inconsistent with the data presented here.

Javel (1981) and Javel *et al.* (1983) have argued that rate suppression and synchrony suppression are related measures. They also conclude that the hair cell detection stage is the most likely site of the suppression effect. How can their results and our conclusions be brought into an agreement?

Our measure, by its nature, must bound from above all other rate suppression threshold measures since we require the excitor rate to be suppressed to near the spontaneous rate. Thus our measure is a more conservative measure. It is hard to imagine how the addition of a subthreshold suppressor tone could drive a superthreshold tone response to its undriven rate if the mechanism is in the hair cell as concluded by Javel. On the other hand, perhaps rate is a poor (insensitive) measure. It was shown by Johnson (1974) and by Javel (1981) that the synchrony threshold is about 14 dB (on the average) below the rate threshold. Thus it would seem that our STC must lie very close to, or just above, the synchrony threshold. In Figs. 14 and 15 we show data which directly address this question. In Fig. 14(a) we show an FTC for a low threshold, high-frequency unit ($f_{CF} = 6800$ Hz). While a continuous CF tone was present, we presented a periodic tone burst at a frequency of 450 Hz at six different levels, and we generated a neural PST histogram. Each PST histogram, along with its Fourier transform, is shown in Fig. 14(b). In the upper panels the tone burst has no effect. At the level of the third panel from the top (with the tone burst at 64 dB SPL), the unit weakly begins to phase lock to the suppressor tone. In the bottom panel the unit responds strongly to the suppressor tone envelope, but has no phase locked component at all (since there are no spikes, there can be no synchrony) while the tone burst is on. At no level is the synchrony of the 420-Hz suppressor strong. In the right-hand family of panels, the synchrony is plotted on a log % scale. In Fig. 15(a) and (b) we show an example where the rate does not go to zero, and where no synchrony component is present at the suppressor frequency (in this case $f_s = 420$ Hz and $f_{CF} = 3174$ Hz).

We have found little suppression in PST (post-stimulus time) period histograms built in the presence of a suppressor above CF and outside of the FTC. The units for which we look most carefully for suppression above CF had low thresholds. Thus damage is not a likely cause for this lack of suppression above CF. In fact, one possible explanation might be that we usually restrict our measurements to low threshold units. On those few occasions, when we measured the suppression for high threshold units, we did see suppression above CF. In Fig. 15(c) the suppression is easily seen. However, since the rate was too high during the suppressed interval to satisfy the spontaneous suppression threshold criterion, no suppression was found by our procedure for this case above CF.

Our threshold paradigm is more conservative than Schmiedt's in that we search for a suppressor amplitude that decreases the firing rate due to the excitor to one spike (per 50 ms) above spontaneous, whereas Schmiedt (1982) searched for the amplitude of a suppressor (scanning from low amplitude to high—his approach to avoiding the two-valuedness in the level-rate curve, Fig. 11) that decreased the firing rate due to the excitor by just less than one spike (per 50 ms). His measure, of course, is guaranteed to show lower "suppression thresholds." Hence, while our measure of suppression above CF shows little effect, it is not necessarily inconsistent with the results of Schmiedt (1982) or Abbas and Sachs (1976).

We looked at the amount of suppression (elevation of the CF threshold) as a function of the suppressor level and we found slopes ranging from 1 dB/dB–3 dB/dB. Units with high thresholds showed a larger slope than units having low thresholds. We feel that more measurements are needed to properly establish these level dependences.

Finally, for low threshold units having their CFs below 1 kHz, we saw little or no two-tone suppression effect. A simple equivalent way of stating this fact was to observe that for these units, the below CF response threshold was always below the fixed suppression threshold values of 60–80 dB SPL. If the FTC threshold was above this range (namely, the unit was one of the low-spontaneous, high-threshold units), then two-tone suppression was observed.

ACKNOWLEDGMENTS

The hospitality of Professor Shyam Khanna, Director of Fowler Memorial Labs, Columbia University, is greatly appreciated. All of the live animal experiments were done at Fowler. Surgical preparation of several of the animals was done by Martha Galley and by Brian Trainor. Much support was received from Dr. David Berkley and very helpful discussions were had with Dr. Joseph Hall of AT&T Bell Laboratories. For part of these studies, PFF was supported with an NSF Science Faculty Fellowship.

Abbas, P. J., and Sachs, M. B. (1976). "Two-tone suppression in auditory-nerve fibers: Extension of a stimulus-response relationship," J. Acoust. Soc. Am. **59**, 112–122.

Allen, J. B. (1981). "Neural tuning thresholds in the presence of a second subthreshold tone," J. Acoust. Soc. Am. Suppl. 1 **69**, S53.

Allen, J. B. (1983). "Magnitude and phase frequency response to single tones in the auditory nerve," J. Acoust. Soc. Am. **73**, 2071–2092.

Buunen, T. J. F., ten Kate, J. H., Raatgever, J., and Bilsen, F. A. (1977). "Combined psychophysical and electrophysical study on the role of combination tones in the perception of phase changes," J. Acoust. Soc. Am. **61**, 508–519.

Buunen, T. J. F., and Rhode, W. J. (1978). "Responses of fibers in the cat's auditory nerve to the cubic difference tone," J. Acoust. Soc. Am. **64**, 772–781.

Fox, P., Hall, A. D., and Schryer, N. L. (1976). "Computing Science Technical Report #47—The Port Mathematical Subroutine Library," FORTRAN code and documentation available from Western Electric Co., Patent Licensing, P. O. Box 20046, Greensboro, NC 27420.

Goldstein, J. L. (1966). "Auditory nonlinearity," J. Acoust. Soc. Am. 41, 676–689.

Goldstein, J. L., Buchsbaum, G., and Furst, M. (1978). "Compatibility between psychophysical and physiological measurements of aural combination tones," J. Acoust. Soc. Am. 63, 474–485.

Goldstein, J. L., and Kiang, N. Y. S. (1968). "Neural correlates of the aural combination tones," Proc. IEEE 56, 981–992.

Hall, J. L. (1981). "Observations on a nonlinear model for motion of the basilar membrane," *Hearing Research and Theory* (Academic, New York), Vol. 1, pp. 1–61.

Hall, J. L. (1974). "Two-tone distortion products in a nonlinear model of the basilar membrane," J. Acoust. Soc. Am. 56, 1818–1828.

Javel, E. (1981). "Suppression of auditory nerve responses. I: Temporal analysis, intensity effects, and suppression contours," J. Acoust. Soc. Am. 69, 1735–1745.

Javel, E., McGee, J. Walsh, E. J., Farley, G. R., and Gorga, M. P. (1983). "Suppression of auditory nerve responses. II. Suppression thresholds and growth, iso-suppression contours," J. Acoust. Soc. Am. 74, 801–813.

Johnson, D. H. (1974). "The response of single auditory-nerve fibers in the cat to single tones: synchrony and average discharge rate," Ph. D. thesis, M. I. T., Cambridge, MA.

Kaiser, J. F. (1966). "Digital filters," in *System Analysis by Digital Computer*, edited by F. F. Kuo and J. F. Kaiser (Wiley, New York), Chap. 7. Program code to implement Kaiser and other windows are in *Programs for Digital Signal Processing*, edited by Digital Signal Processing Committee (IEEE, New York, 1979), Chap. 5.

Kim, D. O., Molnar, C. C., and Matthews, J. W. (1980). "Cochlear mechanics: Nonlinear behavior in two-tone response as reflected in cochlear-nerve-fiber responses and in ear-canal sound pressure," J. Acoust. Soc. Am. 67, 1704–1721.

Kim, D. O. (1980). "Cochlear mechanics: Implications of electrophysiological and acoustical observations," Hear. Res. 2, 297–317.

Liberman, M. C. (1978). "Auditory-nerve response from cats raised in a low-noise chamber," J. Acoust. Soc. Am. 63, 442–455.

Liberman, M. C. (1982). "The cochlear frequency map for the cat: Labeling auditory-nerve fibers of known characteristic frequency," J. Acoust. Soc. Am. 72, 1441–1449.

Matthews, J. W. (1983). "Modeling reverse middle ear transmission of acoustic distortion signals," in *Mechanics of Hearing*, edited by E. de Boer and M. A. Viergever (Delft U. P., Delft, The Netherlands), pp. 11–18.

Mountain, D. C. (1980). "Change in endolymphatic potential and crossed olivocochlear bundle stimulation alter cochlear mechanics," Science 210, 71–72.

Nedzselnitsky, V. (1974). "Measurements of sound pressure in the cochlear of anesthetized cats," in *Facts and Models in Hearing*, edited by E. Zwicker and E. Terhardt (Springer-Verlag, New York).

Rhode, W. (1978). "Some observations on cochlear mechanics," J. Acoust. Soc. Am. 64, 158–176.

Schmiedt, R. A. (1982). "Boundaries of two-tone rate suppression of cochlear-nerve activity," Hear. Res. 7, 335–351.

Siegel, J. H., and Kim, D. O. (1982). "Efferent neural control of cochlear mechanics? Olivocochlear bundle simulation affects cochlear biomechanical nonlinearity," Hear. Res. 6, 171–182.

Sokolich, W. G. (1977). "Improved acoustic system for auditory research," J. Acoust. Soc. Am. Suppl. 1 62, S12.

Smoorenburg, G. F., Gibson, M. M., Kitzes, L. M., Rose, J. E., and Hind, J. E. (1976). "Correlates of combination tones observed in the response of neutrons in the anteroventral cochlear nucleus of the cat," J. Acoust. Soc. Am. 59, 945–962.

Weiner, D. D., and Spina, J. E. (1980). *Sinusoidal Analysis and Modeling of Weakly Nonlinear Circuits* (Van Nostrand, New York), Chap. 4.

Zurek, P. M., Clark, W. W., and Kim, D. O. (1982). "The behavior of acoustic distortion products in the ear canals of chinchillas with normal and damaged ears," J. Acoust. Soc. Am. 72, 774–781.

Zwicker, E. (1981). "Cubic difference tone level and phase dependence on frequency and level of primaries," In *Psychophysical, Physiological and Behavioral Studies in Hearing*, edited by G. van den Brink and F. A. Bilsen (Delft U. P., Delft, The Netherlands).

Nonlinear phenomena as observed in the ear canal and at the auditory nerve

P. F. Fahey, and J. B. Allen

Citation: The Journal of the Acoustical Society of America **77**, 599 (1985); doi: 10.1121/1.391878
View online: https://doi.org/10.1121/1.391878
View Table of Contents: http://asa.scitation.org/toc/jas/77/2
Published by the Acoustical Society of America